Fractal dimension analysis for robust ultrasonic non-destructive evaluation (NDE) of coarse grained materials

Minghui Li, and Gordon Hayward

Fractal Dimension Analysis for Robust Ultrasonic Non-Destructive Evaluation (NDE) of Coarse Grained Materials

Minghui Li [1, a)] and Gordon Hayward [2]

[1]*School of Engineering, University of Glasgow, Glasgow G12 8QQ, United Kingdom*
[2]*Alba Ultrasound, Unit 1, Block 3, Todd Campus, Glasgow G20 0XA, United Kingdom*

[a)]Corresponding author: minghui.li@ieee.org

Abstract. Over the recent decades, there has been a growing demand on reliable and robust non-destructive evaluation (NDE) of structures and components made from coarse grained materials such as alloys, stainless steels, carbon-reinforced composites and concrete; however, when inspected using ultrasound, the flaw echoes are usually contaminated by high-level, time-invariant, and correlated grain noise originating from the microstructure and grain boundaries, leading to pretty low signal-to-noise ratio (SNR) and the flaw information being obscured or completely hidden by the grain noise. In this paper, the fractal dimension analysis of the A-scan echoes is investigated as a measure of complexity of the time series to distinguish the echoes originating from the real defects and the grain noise, and then the normalized fractal dimension coefficients are applied to the amplitudes as the weighting factor to enhance the SNR and defect detection. Experiments on industrial samples of the mild steel and the stainless steel are conducted and the results confirm the great benefits of the method.

INTRODUCTION

Robust inspection of coarse grained materials is a challenging yet essential problem in ultrasonic non-destructive evaluation (NDE). Such materials as stainless steels, alloys, carbon-reinforced composites and concrete are widely used in a variety of industrial sectors like aerospace, energy, oil and gas, nuclear, and transportation. There is a growing demand on reliable and robust inspection of structures and components made from these materials; however, when inspected using ultrasound, the flaw echoes are usually contaminated by high-level, time-invariant, and correlated grain noise originating from the microstructure and grain boundaries, leading to quite low SNR and the flaw information being obscured or lost completely. The phenomenon becomes even worse when the size of the material grains is coarse, in terms of the wavelength of the ultrasound in consideration.

The problem received considerable attention from the NDE community in recent decades but only limited degree of success has been achieved, and several techniques were investigated to enhance the flaw detection or reduce the clutter noise by exploring either the spatial diversity across the array aperture [1-4], or the temporal-spectral characteristics and signatures of the broadband ultrasonic signals [5-12]. Array beamforming is widely used in radar and communication systems for spatial filtering and diversity processing [13-17]. In order to enhance the SNR of ultrasonic NDE, transducer array beamforming filters the data in the spatial domain by retaining the energy coming from the array focal point, while minimizing the interference from all the other locations [1-2]. The coherence factoring method [3] computes the factor of the energy of the coherent sum obtained in the delay-and-sum operation to the total incoherent energy and uses it to weight the amplitude. The techniques exploring the temporal-spectral characteristics of the ultrasonic signals include split spectrum processing and matched filtering. The split spectrum processing method [5] obtains a frequency-diverse ensemble of narrowband signals from the broadband ultrasonic echoes through a filter bank, and then recombines them to determine if the signal originates from a real defect or grain boundaries. The matched filtering technique [8-9] computes the optimal parameters in the filter response through maximizing the SNR improvement over a set of training signals captured from the test sample, and then uses the signal matching concept to detect the echoes from a real defect [6-7].

In this paper, a novel approach based on the fractal dimension analysis of the broadband ultrasound A-scan waveform is investigated to distinguish between the echoes originating from legitimate reflectors and the material microstructure grain noise. The concept of fractal dimension is a generalization of the Euclidean dimension that reflects the complexity of the self-similar structure of an object or time series. The fractal dimension has been used for analysis and quantification of complicated biomedical signals such as ECG and EEG [18-20], and more recently in the field of tissue characterization in medical ultrasound diagnosis [21]. To estimate the fractal dimension of a time series, the signal is decomposed into different scales and then the signal complexity is evaluated. When the method is applied to the ultrasonic A-scan waveforms in phased array systems, the echo signals are firstly pre-processed with the delay-and-sum operation, and then the synthesized echoes are divided into segments. The fractal dimension estimation is applied to the segments one by one, to determine if the portion of echoes originates from a real defect or grain boundaries.

The technique is validated with experiments on a solid mild steel sample and an austenitic stainless steel sample with a 128-element 5MHz transducer array, and the total focusing method (TFM) is utilized to create the images. It has been observed that the echo segments originating from the legitimate reflectors such as the side-drilled holes and the back-wall of the specimen demonstrate the fractal dimension coefficients different from those of grain noise, and the TFM images are greatly improved when the amplitudes are weighted using the fractal dimension coefficients as a weighting factor. As a result, the echoes from the real reflectors such as cracks, flaws or the back-wall are well maintained while the clutter noise from the grain boundaries is greatly reduced. The additional computational cost in evaluation of the fractal dimension is moderate or low, which makes it suitable for rapid applications.

FRACTAL DIMENSION ESTIMATION AND ANALYSIS

In this section, we illustrate how to estimate the fractal dimension of an echo signal (A-scan time series), and present the related algorithms and equations. In a conventional ultrasonic testing system with a single transducer, individual A-scan echoes are collected at different locations. While in more advanced transducer array based systems, focusing is firstly applied to the array output data as a way of pre-processing to focus the beam on a particular location in consideration. The A-scan echoes or the synthesized echoes are then divided into segments with the length of N samples; these N samples are assumed to contain the information of the internal structure of a particular area of the insonified media. Assume that the echoes originating from legitimate reflectors and grain noise produce waveforms with different shape, pattern or complexity; the fractal dimension of the segment is computed as a measure or index of complexity to capture the difference between them, and further reveal and illustrate the intrinsic characteristics of this particular area under investigation.

In literature, there are several algorithms available for estimation of the fractal dimension of a time series [22-24]. The approach proposed by Higuchi [22] is proven to be stable and accurate to estimate the fractal dimension of time series even when the signal is short with only limited samples. This property is extremely important for the segment-based analysis proposed in this work, in which the echoes are divided into short segments. Higuchi's estimation algorithm is straightforward to implement. In short, the echo segment is first decomposed into different scales, the algorithm then computes the mean length of the signal at different scales and plots a log-log graph of length versus scale, and finally measures the slope of the linear fit of this graph as the estimate of the fractal dimension of the segment.

Consider a N sample time series (segment of echo data samples), $\{x(1), x(2), ..., x(N)\}$. Firstly, construct k new time series in the following form [22]

$$x_k^m \; : \; \left\{ x(m), \; x(m+k), \; x(m+2k), \; ..., \; x\left(m + \left\lfloor \frac{N-m}{k} \right\rfloor \cdot k\right)\right\}, \tag{1}$$

where both k and m are integers, $k < N$ determines the scale, $m = 1, 2, ..., k$, and $\lfloor \cdot \rfloor$ means rounding down to the nearest integer.

The length $L_m(k)$ of each time series x_k^m is defined as

$$L_m(k) = \frac{1}{k} \cdot \frac{N-1}{\left\lfloor \frac{N-m}{k} \right\rfloor \cdot k} \cdot \sum_{i=1}^{\left\lfloor \frac{N-m}{k} \right\rfloor} |x(m+ik) - x(m+(i-1)\cdot k)|, \tag{2}$$

The mean length of the time series at scale k is defined as

$$L(k) = \frac{1}{k}\sum L_m(k). \tag{3}$$

The procedure is repeated for each k, for $1 \leq k \leq K_{max}$. A line is fitted to values of $ln\big(L(k)\big)$ versus $ln(1/k)$, and the slope of this line is considered to be the fractal dimension of the time series $\{x(1), x(2), \ldots, x(N)\}$.

In the method, K_{max} is a design parameter in estimation of the fractal dimension, and the optimal value is determined by the number of samples N in the segment and the intrinsic nature of the time series. In the experiments of the following section, K_{max} is pre-defined, and we have been determining the best value of K_{max} with trails and errors. The method to determining the optimal value of K_{max} is being investigated.

EXPERIMENTAL VERIFICATION

In this section, we demonstrate the implementation and utilization of the fractal dimension coefficients of the A-scan echoes as a measure of the complexity of the time series in order to 1) capture the difference between the defect signals and grain noise, 2) evaluate the performance of fractal dimension analysis for ultrasonic NDE imaging and defect detection, and 3) compare it with the gold-standard TFM technique [1].

The experimental apparatus employed in this work consists of the test sample, the ultrasound array transducer, the phased array control system, and a personal computer for excitation, data collection and signal processing. A 128-element transducer array with 0.7 mm element pitch and 5 MHz central frequency (Vermon, Tours, France) is employed in contact with the test sample upper surface with gel coupling, as shown in Fig. 1(a). An OPEN ultrasonic phased array control system (LeCouer, Chuelles, France), with 128 independent parallel channels and 16-bit resolution is connected with the transducer array for excitation and data acquisition, as shown in Fig. 1(b). A personal computer is then connected to the OPEN system to control the excitation sequence and record the return signals for post signal processing and imaging. A MATLAB (The MathWorks, Natick, MA) routine is developed to implement the Full Matrix Capture (FMC) data acquisition, where each transducer element is excited sequentially and the echoes received by all array elements are recorded [1]. A complete FMC data set is composed of N^2 A-scan waveforms, where N is the number of array elements.

Experiment I

In the first experiment, the test sample is a solid mild steel block with thickness of 60 mm in which multiple 3 mm diameter cylindrical side holes are drilled at different lateral positions and depths, as shown in Fig. 1(a). The sampling rate of the phased array controller is set to 40 MHz. The echoes are pre-focused and then divided into segments with a length of 5 wavelengths, and the parameter K_{max} used in fractal dimension estimation is pre-defined to be 16.
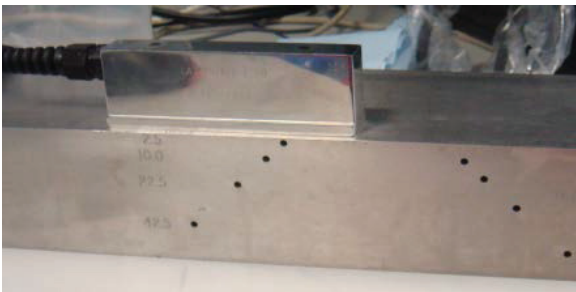
(a)   (b)

FIGURE 1. Experimental apparatus. (a) Transducer array and test sample,
and (b) OPEN phased array control system.

The fractal dimension of the echo segment is estimated using equations (1-3) and then normalized, which is illustrated in Fig. 2. As shown in Fig. 2, the echoes originating from the side-drilled holes produce higher (normalized) fractal dimension coefficients, and grain noise produces relatively lower fractal dimension coefficients, due to the difference in the nature, pattern and complexity of the echo segments. From the illustration of the fractal dimension coefficients in Fig. 2, it is evident that the 3 side-drilled holes can be readily distinguished.

The data are further processed for imaging. Fig. 3(a) shows the image obtained with the Total Focusing Method (TFM) [1] using the original FMC data set. To form the image in Fig. 3(b), firstly, the fractal dimensions of the A-scan echoes are estimated segment by segment, and then the normalized fractal dimension coefficient is multiplied with the amplitudes of the TFM image element by element as a weighting factor. As can be seen from Fig. 3, in the original TFM image of Fig. 3(a), the 3 side-drilled holes are visible, and there is some grain noise, which demonstrates a somewhat homogeneous feature due to the finer grain size. While in the image of Fig. 3(b), which is weighted with the fractal dimension coefficients, the grain noise is significantly reduced and the side-drilled holes are better defined. As a result, the imaging and defect detection are enhanced.
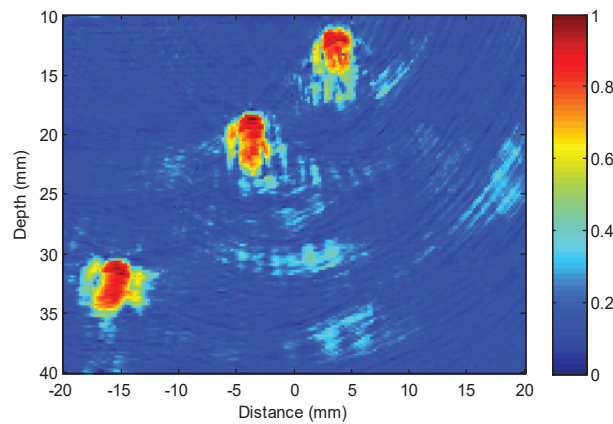

FIGURE 2. Normalized fractal dimension coefficients of mild steel block.
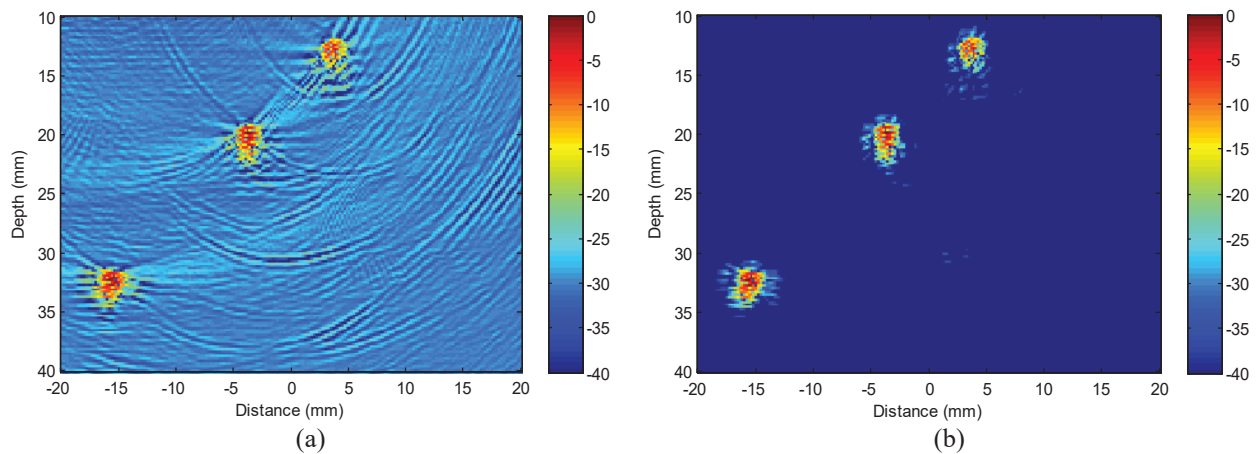

FIGURE 3. Images of mild steel block. (a) TFM with original FMC data set, and (b) TFM image weighted with normalized fractal dimension coefficients.

Experiment II

A test sample from a coal-fueled power plant generator end ring with a thickness of around 55 mm made of austenitic stainless steel is investigated in the second experiment. The stainless steel material is widely used in a variety of key industrial sectors like Energy, Oil and Gas, Transportation, and Nuclear for components such as ducting, combustion cans and transition liner. The FMC data set is recorded at a sampling rate of 100 MHz, and each A-scan waveform is properly band-pass filtered to remove the DC drift and high frequency noise before pre-focusing. Due to the size of microstructure grains, stainless steel is demonstrated to be highly scattering to the 5 MHz ultrasound, and results in dominant and significant grain noise and quite low SNR. In this experiment, the length of segments N remains to be 5 wavelengths, and the parameter K_{max} is pre-defined to be 16.

Fig. 4(a) illustrates the normalized fractal dimension coefficients of the echo waveforms which are estimated using equations (1-3) and then normalized. Figure 4(b) shows the image obtained with the TFM method using the original FMC data set, and Fig 4(c) demonstrates the TFM image weighted with the normalized fractal dimension coefficients. As shown in Fig. 4, the back-wall echoes demonstrate higher values of the normalized fractal dimension coefficients, based on that it is potentially able to distinguish defects (legitimate reflectors) from grain noise. In the original TFM image, the grain noise is significant due to grain boundaries and the internal structure of stainless steel. The back-wall reflection is visible, but the SNR is not high. When the fractal dimension coefficients
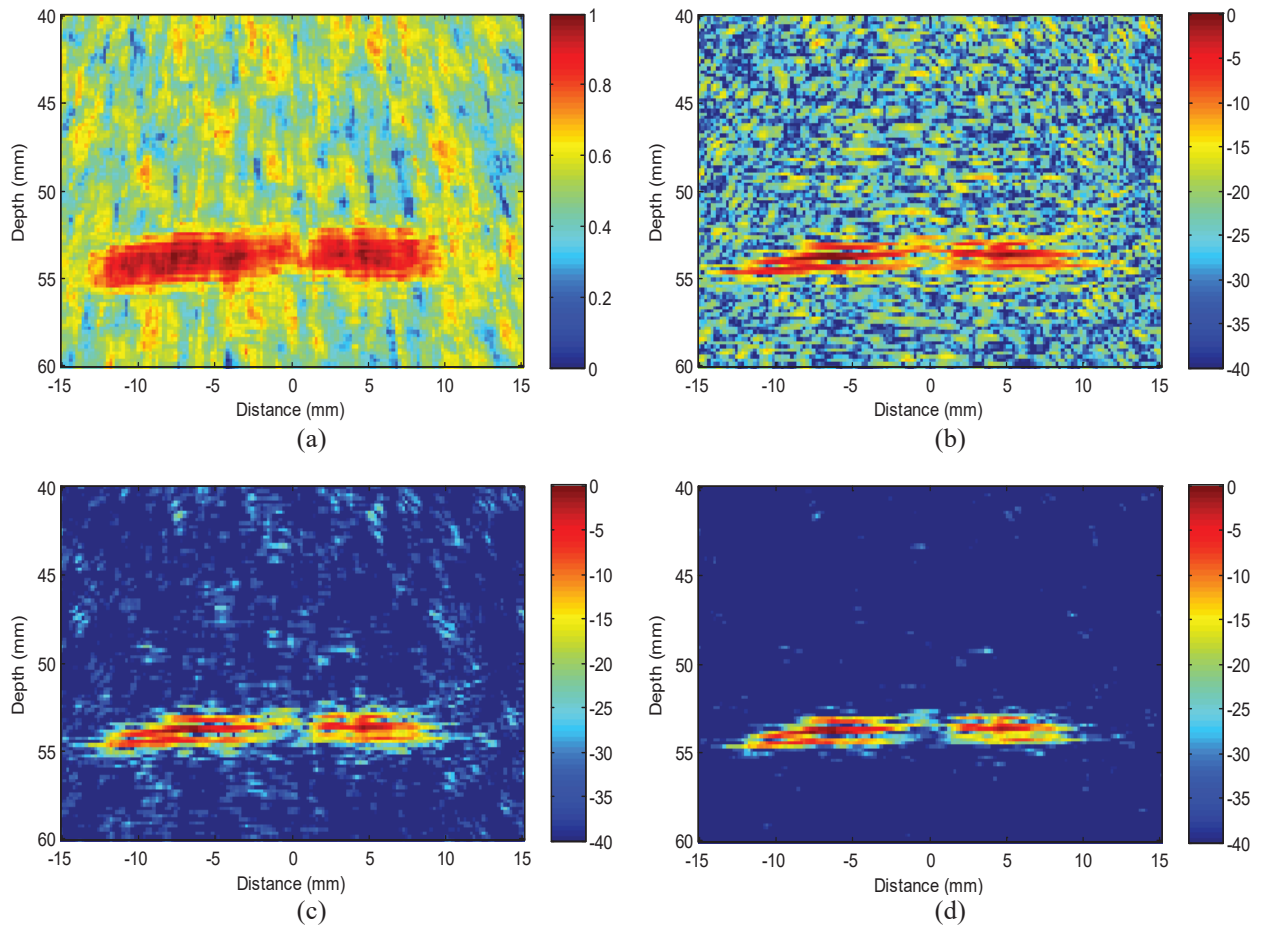

FIGURE 4. Images of austenitic stainless steel sample. (a) Normalized fractal dimension coefficients, (b) TFM with original FMC data set, (c) TFM image weighted with normalized fractal dimension coefficients, and (d) TFM image processed with both fractal dimension analysis and adaptive beamforming.

are applied as a weighting factor to the amplitudes in Fig. 4(c), it is evident that the grain noise is significantly reduced compared to the original image of Fig. 4(b); in the meantime, the reflection from the back-wall is well maintained and defined. It can be seen from Fig. 4, that the defect detection and imaging are greatly enhanced when the fractal dimension analysis is applied to the data.

The fractal dimension analysis is applied to the A-scan waveforms and works in the temporal-spectral domain. On the other hand, a variety of beamforming methods that exploit the spatial diversity and filtering, like the Capon beamforming [1-2], were investigated in the literature. There is a potential to combine these two categories of techniques since they work in different domains and may complement each other for noise reduction and defect detection enhancement. Fig. 4(d) shows the image processed with both the fractal dimension analysis and adaptive Capon beamforming. As comparison to the image in Fig. 4(c), which is only processed with the fractal dimension analysis, it is evident that the clutter noise is further reduced, and the back-wall reflection is greatly enhanced in terms of the strength as well as the visible lateral length, due to exploiting both the temporal and spatial information.

CONCLUSIONS AND FUTURE WORK

This paper has presented a robust method to ultrasonic NDE of coarse grain materials based on the fractal dimension analysis of the A-scan echo waveforms. The fractal dimensions of the echoes are computed as an index of complexity of the time series in order to capture the difference between the signals originating from real defects and grain noise. The normalized fractal dimension coefficients can then be utilized as a weighting factor to weight the amplitudes in order to enhance the defect detection and imaging. Experiments on industrial samples of the solid mild steel and the stainless steel are conducted and the results confirm the advantages and robustness of the approach. The parameter K_{max} has been chosen as a design parameter and pre-determined in this work based on trials and errors. The determination of an adaptive and optimal K_{max} will be considered in the future improvement, and the enhanced version will be investigated for defect detection and further defect characterization on a variety of industrial samples of alloys, composites and stainless steel.

REFERENCES

1. M. Li and G. Hayward, "Ultrasound non-destructive evaluation (NDE) imaging with transducer arrays and adaptive processing," *Sensors,* **12**:1, 42-54, (2012).
2. M. Li, G. Hayward and B. He, "Adaptive array processing for ultrasonic non-destructive evaluation," *2011 IEEE International Ultrasonics Symposium (IUS) Proceedings*, pp. 2029-2032, (2011).
3. P.-C. Li and M.-L. Li, "Adaptive imaging using the generalized coherence factor," *IEEE Transactions on Ultrasonics, Ferroelectrics, and Frequency Control,* **50**:2, 128-141, (2003).
4. T. Lardner, M. Li, R. Gongzhang and A. Gachagan, "A new speckle noise suppression technique using cross-correlation of array subapertures in ultrasonic NDE of coarse grain materials," *Review of Progress in QNDE* (Vol. 32), (eds.) D. O. Thompson and D. E. Chimenti, *AIP Conference Proc*., **1511**(1), pp. 865-871, (2013).
5. K. Ho, M. Li, R. O'Leary and A. Gachagan, "Application of frequency compounding to ultrasonic signals for the NDE of concrete," Review of Progress in QNDE (Vol. 31), (eds.) D. O. Thompson and D. E. Chimenti, *AIP Conference Proc*., **1430**, pp.1508-1515, (2012).
6. K. Srinivasan, C. P. Chiou, and R. B. Thompson, "Ultrasonic flaw detection using signal matching techniques," Review of Progress in QNDE (Vol. 14), (eds.) D. O. Thompson and D. E. Chimenti, *AIP Conf Proceedings*, pp. 711-718 (1995).
7. N. Ruiz-Reyes, P. Vera-Candeas, J. Curpian-Alonso, R. Mata-Campos, and J. C. Cuevas-Martinez, "New matching pursuit-based algorithm for SNR improvement in ultrasonic NDT," *NDT&E International,* **38**(6), pp. 453-458, (2005).
8. M. Li and G. Hayward, "Optimal matched filter design for ultrasonic NDE of coarse grain materials," Review of Progress in QNDE (Vol. 35), (eds.) D. E. Chimenti and L. J. Bond, *AIP Conf. Proceedings*, **1706**, 020011, 1-9, (2016).
9. M. Li and G. Hayward, "A rapid approach to speckle noise reduction in ultrasonic non-destructive evaluation using matched filters," *IEEE International Ultrasonics Symposium (IUS) Proceedings*, pp. 45-48, (2014).
10. R. Gongzhang, M. Li, B. Xiao, T. Lardner and A. Gachagan, "Robust frequency diversity based algorithm for clutter noise reduction of ultrasonic signals using multiple sub-spectrum phase coherence," Review of Progress in QNDE, (Vol. 33), eds. D. E. Chimenti, L. J. Bond and D. O. Thompson, *AIP Conf. Proceedings*, **1581**, pp. 1948-1955, Melville, NY, (2014).

11. B. Xiao, M. Li, R. Gongzhang, R. O'Leary and A. Gachagan, "Image de-noising via spectral distribution similarity analysis for ultrasonic non-destructive evaluation," Review of Progress in QNDE (Vol. 33), (eds.) D. E. Chimenti, L, J. Bond and D. O. Thompson, *AIP Conf. Proceedings*, **1581**, pp. 1941-1947, (2014).

12. R. Gongzhang, M. Li, T. Lardner and A. Gachagan, "Robust defect detection in ultrasonic nondestructive evaluation (NDE) of difficult materials," *IEEE International Ultrasonics Symposium Proceedings*, (Dresden, Germany), pp. 467-470, (2012).

13. M. Li and Y. Lu, "Optimal direction finding in unknown noise environments using antenna arrays in wireless sensor networks," *7th International Conference on Intelligent Transportation Systems Telecommunications Proceedings*, (Sophia Antipolis, France), pp. 332-337, (2007).

14. M. Li and Y. Lu, "Maximum likelihood DOA estimation in unknown colored noise fields," *IEEE Transactions on Aerospace and Electronic System,s* **44**:3, pp. 1079-1090, (2008).

15. M. Li and Y. Lu, "Improving the performance of GA-ML DOA estimator with a resampling scheme," *Signal Processing,* **84**:10, pp. 1813-1822, (2004).

16. M. Li and Y. Lu, "Source bearing and steering-vector estimation using partially calibrated arrays," *IEEE Transactions on Aerospace and Electronic Systems,* **45**:4, 1361-1372, (2009).

17. M. Li and Y. Lu, "Angle-of-arrival estimation for localization and communication in wireless networks,"*16th European Signal Processing Conference Proceedings*, (Lausanne, Switzerland), pp. 1-5, (2008).

18. F. Beckers, B. Verheyden, K. Couckuyt, and A. Aubert, "Fractal dimension in health and heart failure," *Biomedizinische Technik. Biomedical Engineering,* **51**:4, 194-197, (2006).

19. G. Henderson, E. Ifeachor, N. Hudson, C. Goh, N. Outram, C. D. Percio, and F. Vecchio, "Development and assessment of methods for detecting dementia using the human electroencephalogram," *IEEE Transactions on Biomedical Engineering,* **53**:8, 1557-1568, (2006).

20. A. Accardo, M. Affinito, M. Carrozzi, and F. Bouquet, "Use of the fractal dimension for the analysis of electroencephalographic time series," *Biological Cybernetics,* **77**:5, pp. 339-350, (1997).

21. M. Moradi, P. Abolmaesumi, P. Isotalo, D. Siemens, E. Sauerbrei, and P. Mousavi, "Detection of prostate cancer from RF ultrasound echo signals using fractal analysis," in *Proceedings of 28th Annual International Conference of the IEEE Engineering in Medicine and Biology Society*, pp. 2400-2403, (2006).

22. T. Higuchi, "Approach to an irregular time series on the basis of the fractal theory," *Physica D,* **31**:2, pp. 277-283, (1988).

23. M. Katz, "Fractals and the analysis of waveforms," *Computers in Biology and Medicine,* **18**:3,145-156, (1988).

24. R. Esteller, G. Vachtsevanos, J. Echauz, and B. Litt, "A comparison of fractal dimension algorithms," *IEEE Transactions on Circuits and Systems,* **48**:2, pp. 177-183, (2001).